

Band structure and Cl *K* x-ray-absorption near-edge structures of a K_2PdCl_6 crystal

Michihide Kitamura and Shinji Muramatsu

Department of Electrical and Electronic Engineering, Faculty of Engineering, Utsunomiya University, 2753 Ishii-machi, Utsunomiya, Tochigi 321, Japan

(Received 11 December 1989; revised manuscript received 29 March 1990)

The band structure of crystalline K_2PdCl_6 is calculated on the basis of the extended Hückel tight-binding method, using the self-consistent charge for K, Pd, and Cl ions obtained in our previous molecular-orbital (MO) calculations. The calculated partial density of states is compared with available experimental data obtained with use of x-ray spectroscopy. In order to explain multiple structures of the Cl *K* x-ray-absorption spectrum, a multiple-scattering theory is applied using the self-consistent charge. From comparison of both the band structure and multiple-scattering calculations with experiments, it is found that the use of the self-consistent charge (K^+ , $Pd^{1.6+}$, $Cl^{0.6-}$) is crucial. This indicates the significance of electron configurations determined from a MO study for crystals like K_2PdCl_6 .

I. INTRODUCTION

A K_2PdCl_6 crystal can be regarded as $K_2^+Q^{2-}$ (with $Q = PdCl_6$), which adopts a CaF_2 -type arrangement. This crystal is one of the best candidates for cluster calculations, because each octahedral complex $(PdCl_6)^{2-}$ is quite isolated from the other $(PdCl_6)^{2-}$ complexes, K^+ ions being embedded between these complexes, as seen from Fig. 1. On the basis of this observation we have recently carried out molecular-orbital (MO) calculations for the octahedral complex $(PdCl_6)^{2-}$ in crystalline K_2PdCl_6 with a self-consistent-charge extended Hückel (SCCXH) method and demonstrated that experimental features of the x-ray-absorption and -emission spectra for both the Pd and Cl ions are well explained by MO calculations except for structures which follow the first peak in the absorption spectrum.¹ These structures are beyond interpretation in terms of MO theory, and should be analyzed in terms of a multiple-scattering (MS) theory, which has been successfully applied to the x-ray-absorption spectra for many cases by the present authors.²⁻⁸

Very recently, we have studied the band structures of some perovskite-type compounds KMF_3 (where $M = Mn, Fe, Co, Ni, Cu,$ and Zn), applying an extended Hückel tight-binding (XHTB) method,⁹ in which atomic orbitals obtained from first principles are used instead of empirical ones. It has been found that total and partial densities of states obtained by the XHTB method well predict experimental data obtained from ultraviolet photoelectron and x-ray spectroscopies.

In the present paper, we first calculate the band structure of the K_2PdCl_6 crystal using our XHTB method as before and compare the results with experimental x-ray spectra, and then we perform calculations of x-ray-absorption near-edge structures (XANES) on the basis of the MS theory in order to interpret XANES which cannot be explained by the MO scheme. Our intention in the present paper is to summarize studies of the electronic structure of crystalline K_2PdCl_6 based on these three

different approaches, MO, band structure, and MS, all of which are properly applicable to this crystal.

In Sec. II we briefly describe our calculational procedures. In Sec. III A the results for total and partial densities of states are presented. They include results for a hypothetical band-structure calculation, in which the contribution of potassium ions is neglected but keeping the remaining input data, such as crystal structure, the same. These calculated results are compared with experi-

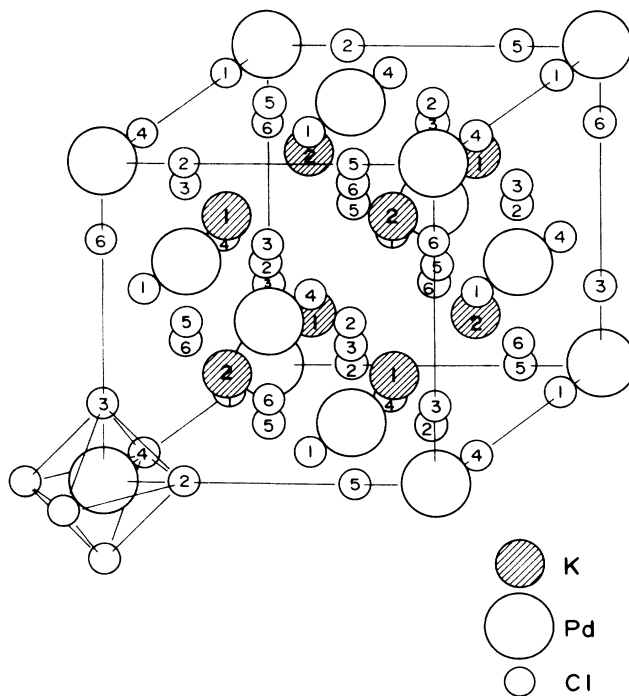


FIG. 1. Unit cell of K_2PdCl_6 crystal. Two different types of potassium ions are denoted by 1 and 2, and six different types of chlorine ions are indicated by 1, 2, 3, 4, 5, and 6. An octahedron is also illustrated.

mental x-ray-absorption and -emission spectra and our previous MO calculations. Cl K XANES spectra calculated with the MS theory for the K_2PdCl_6 are presented and compared with experiment in Sec. III B.

II. CALCULATION

Theoretical details for band-structure calculations based on the XHTB method have been described in our previous paper.⁹ Here, we mention only different points from the previous work for the perovskite-type compounds KMF_3 .

In the K_2PdCl_6 crystal unit cell, the inequivalent sites are K(1), K(2), Pd, Cl(1), Cl(2), Cl(3), Cl(4), Cl(5), and Cl(6) as shown in Fig. 1 and the Brillouin zone is constructed from a fcc Bravais lattice. As the electron configurations for K, Pd, and Cl ions, we adopted $K^+(1s^2 2s^2 2p^6 3s^2 3p^4 s^0)$, $Pd^{1.6+}(1s^2 2s^2 2p^6 3s^2 3p^6 3d^{10} 4s^2 4p^6 4d^{8.3} 5s^{0.06} 5p^{0.04})$, and $Cl^{0.6-}(1s^2 2s^2 2p^6 3s^2 3p^5.6)$, whose configurations have been obtained from the MO calculations for an octahedron $(PdCl_6)^{2-}$ in the K_2PdCl_6 crystal on the basis of the SCCXH method, by taking $G = 1.75$.¹ Here, G is an adjustable parameter used in the Wolfsberg-Helmholtz approximation¹⁰ for the evaluation of the Hamiltonian matrix element. In the present paper, we used 1.75 as the value of G . The atomic orbitals used to calculate the band structures are $3p$ and $4s$ orbitals of K^+ , $4d$, $5s$, and $5p$ orbitals of $Pd^{1.6+}$, and $3s$ and $3p$ orbitals of $Cl^{0.6-}$, which are obtained from the self-consistent-field (SCF) calculations^{1,3-9} for the respective ions. The size of the resulting Hermitian matrices is 41.

The calculations of the Cl K XANES spectra based on the MS theory within the MT approximation consist of three parts. The first part is the SCF calculations for K, Pd, Cl, and K x-ray-absorbing Cl ions. In order to see the effect of charge transfer on the XANES spectra, the SCF calculations for formal charge $Pd^{4+}(1s^2 2s^2 2p^6 3s^2 3p^6 3d^{10} 4s^2 4p^6 4d^6)$ and $Cl^-(1s^2 2s^2 2p^6 3s^2 3p^6)$ were also carried out. The electron configurations of the K x-ray-absorbing Cl ions are $Cl^{0.6-}(1s^1 2s^2 2p^6 3s^2 3p^5.6 4p^1)$ for the self-consistent charge and $Cl^-(1s^1 2s^2 2p^6 3s^2 3p^6 4p^1)$ for the formal charge. The SCF calculations are carried out following a prescription of Herman and Skillman¹¹ and using Schwarz's exchange parameter¹² for the exchange correction. The second part is the construction of crystal potentials by use of the atomic data obtained in the first part. In this construction the Madelung correction due to the charge transfer is taken into account exactly by using Evjen's method.¹³ The crystal potentials are constructed within the MT approximation by using the same procedure as in our previous work.⁴ Here, we mention how the MT radius (R) and the MT zero (V_0) characterizing the MT potentials were determined. In our previous paper for the perovskite-type compounds,⁵ we showed that the position and the energy of the point where the Madelung-corrected potentials $V^c(r)$ cross can be used for the R and the first value of V_0 but in the three component crystals the MT parameters cannot be uniquely determined. We have chosen the MT radii for Pd and Cl ions in such a way that the Madelung-

corrected potentials for Pd and Cl ions cross, namely, R_{Pd} plus R_{Cl} is equal to ua_0 , and we have chosen the R_K as $0.2a_0$ by referring to the MT radius for the potassium ions used in the XANES calculations of the perovskite-type compounds.⁵ We have carefully checked that the calculated XANES spectra do not strongly depend on a choice of the R_K . Here, a_0 is the lattice constant (9.74 Å) and u is the value of u in the table of Wyckoff.¹⁴ We used 0.243 as the value of u , which is the same as in our previous work,¹ and adopted $V_K^c(R_K)$ as the value of V_0 . The final part is to carry out the calculations of XANES on the basis of the MS theory.² In the final calculations, we adopted the condition that the cluster taken into account in the MS calculations is made of 48 atoms and the maximum angular momentum (l_{max}) is set to 2. Therefore, the size of the supermatrix defined in Eq. (3a) in Ref. 2 is 432. The MS calculation corresponding to $l_{max}=3$, in which the size of the supermatrix is 768, was not carried out because of memory area available in the computer and the computation time. The effect of partial f waves, however, will be discussed from the viewpoint of scattering cross sections.

III. RESULTS AND DISCUSSION

In this section we present results for the total and partial densities of states and calculated Cl K XANES spectra. Available experimental data which can be compared with our calculations are the spectra for Pd $L\beta_{2,15}$ emission,¹ Pd L_3 absorption,¹ Cl $K\beta$ emission,¹ and Cl K absorption.¹ These spectra are discussed in Sec. III A in connection with the partial density of states obtained from the band-structure calculation, along with general properties of the band structure, and in Sec. III B the Cl K absorption spectrum is discussed again in connection with Cl K XANES calculation.

A. Band structure

The calculated results for the total density of states (TDOS) are shown in Figs. 2(a) and 2(b). Figure 2(b) indicates the results obtained by neglecting the K^+ ions, and also indicates the MO levels calculated by the SCCXH method in our previous work.¹ We denote the partial densities of states (PDOS) for $3p$ and $4s$ orbitals of K, the $5p$ orbital of Pd, $4d$ and $5s$ orbitals of Pd, the $3s$ orbital of Cl, and the $3p$ orbital of Cl by $P_{3p}^{(K)}$, $P_{4s}^{(K)}$, $P_{5p}^{(Pd)}$, $P_{4d}^{(Pd)}$, $P_{5s}^{(Pd)}$, $P_{3s}^{(Cl)}$, and $P_{3p}^{(Cl)}$, respectively. Since the $P_{4d}^{(Pd)}$, $P_{5s}^{(Pd)}$, and $P_{3p}^{(Cl)}$ are necessary to a comparison with experiments, we show the $P_{4d}^{(Pd)}$ and $P_{5s}^{(Pd)}$ in Fig. 3 and the $P_{3p}^{(Cl)}$ in Fig. 4. In Fig. 3(a) the experimental Pd $L\beta_{2,15}$ emission (solid curve) and Pd L_3 absorption (dashed curve) spectra are also shown for comparison, and in Fig. 3(b) their MO results are compared with $P_{4d}^{(Pd)}$ and $P_{5s}^{(Pd)}$ obtained without the K^+ ions. In Fig. 4(a) the experimental Cl $K\beta$ emission (solid curve) and Cl K absorption (dashed curve) spectra are compared with the $P_{3p}^{(Cl)}$, and in Fig. 4(b) their MO results are compared with $P_{3p}^{(Cl)}$ obtained without the K^+ ions. We should note that the curves in Figs. 3(a) and 4(a) are drawn in such a way that the

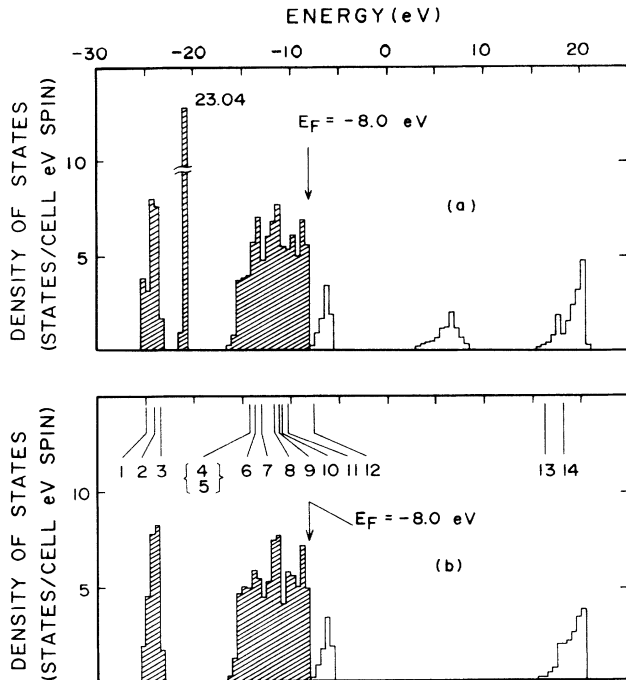


FIG. 2. Total density of states (TDOS) of K_2PdCl_6 . Energy is measured from vacuum level. (a) The TDOS calculated by taking into account $3p$ and $4s$ orbitals of K^+ , $4d$, $5s$, and $5p$ orbitals of $Pd^{1.6+}$, and $3s$ and $3p$ orbitals of $Cl^{0.6-}$ ions, on the basis of the extended Hückel tight-binding (XHTB) method. (b) The TDOS calculated by the XHTB method for a hypothetical crystal, in which K^+ ions are neglected. Molecular-orbital (MO) levels obtained from the MO calculation based on the self-consistent-charge extended Hückel (SCCXH) method are also indicated. The MO levels are denoted by the numbers from 1 to 14, which correspond to $1a_{1g}$, $1t_{1u}$, $1e_g$, $1t_{2g}$, $2a_{1g}$, $2t_{1u}$, $2e_g$, $1t_{2u}$, $2t_{2g}$, $3t_{1u}$, $1t_{1g}$, $3e_g$, $3a_{1g}$, and $4t_{1u}$, respectively.

heights of the most intense peaks of the experimental emission and absorption spectra coincide with those of the respective PDOS's; that the energy of the intense peak of the experimental $Pd L\beta_{2,15}$ and $Cl K\beta$ emission spectra coincide with those of the respective PDOS's of Figs. 3(a) and 4(a). The curves for the MO results in Figs. 3(b) and 4(b) are drawn in such a way that the vacuum levels for the band and MO calculations coincide with each other.

First, let us discuss the TDOS shown in Fig. 2(a). The valence band consists of three parts, lower ($V1$), middle ($V2$), and upper ($V3$) bands, and the conduction band also consists of lower ($C1$), middle ($C2$), and upper ($C3$) bands. The comparison of Figs. 2(a) and 2(b) indicates that the $V2$ and $C2$ bands are originated from K^+ ions. From the results of the $P_{3p}^{(K)}$, $P_{4s}^{(K)}$, and $P_{3p}^{(Cl)}$, it is found that the $V2$ band comes from the $P_{3p}^{(K)}$, and the $C2$ band comes from the $P_{4s}^{(K)}$ and $P_{3p}^{(Cl)}$. From Figs. 4(a) and 4(b), we observe that the PDOS appearing at about 5 eV in the $P_{3p}^{(Cl)}$ is induced by the inclusion of the K^+ ions. Thus, we can ascribe the $V2$ band to $K 3p$ state, and the $C2$ band to $K 4s$ state mixed with $Cl 3p$ state. The $V1$ band

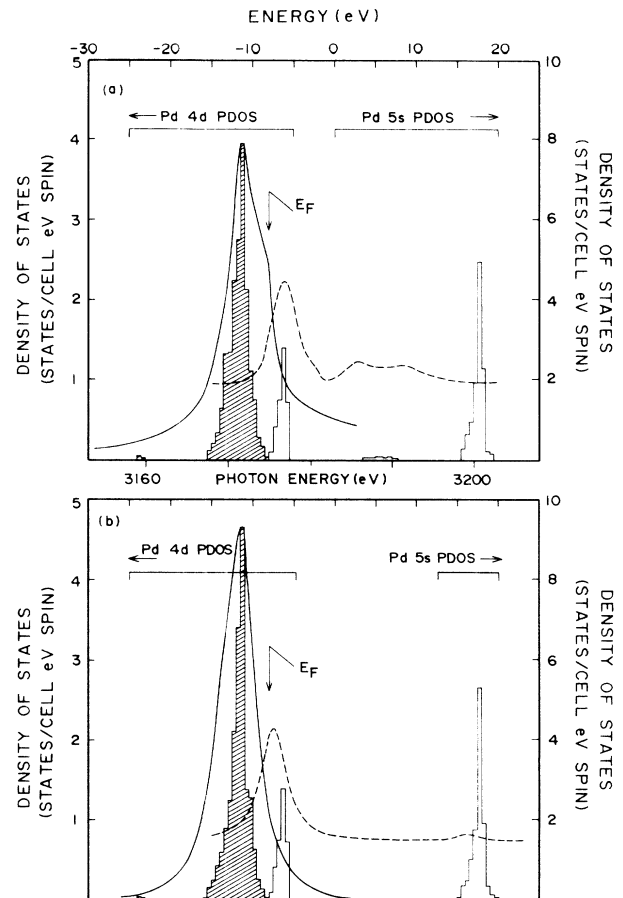


FIG. 3. Partial density of states (PDOS) for $4d$ and $5s$ orbitals of $Pd^{1.6+}$ ion in K_2PdCl_6 as a function of energy measured from vacuum level. $Pd L\beta_{2,15}$ emission (solid curves) and $Pd L_3$ absorption (dashed curves) spectra obtained from the experiment and from the MO calculations based on the SCCXH method are drawn in (a) and (b), respectively. The PDOS illustrated in (b) is the result obtained by neglecting the K^+ ions.

is formed by the $P_{3s}^{(Cl)}$, while the $C3$ band by the $P_{5p}^{(Pd)}$, $P_{5s}^{(Pd)}$, $P_{3s}^{(Cl)}$, and $P_{3p}^{(Cl)}$. The $V3$ and $C1$ bands are separated by the Fermi level from each other, and are formed by the $P_{4d}^{(Pd)}$ [Fig. 3(a)] and $P_{3p}^{(Cl)}$ [Fig. 4(a)].

Next, we shall consider the $P_{4d}^{(Pd)}$, $P_{5s}^{(Pd)}$, and $P_{3p}^{(Cl)}$ shown in Figs. 3(a), 3(b), 4(a), and 4(b), from the viewpoint of the comparison with experiment. The observed $Pd L\beta_{2,15}$ [solid curve in Fig. 3(a)] and $Cl K\beta$ [solid curve in Fig. 4(a)] emission spectra exhibit, respectively, a shoulder and a dip at the high-energy side of the respective main peaks. As pointed out in the previous paper,¹ these structures are due to the effect of self-absorption of the emitted x-ray in the spectral region overlapping with the absorption region. We note that the PDOS to be compared with the experimental $Pd L_3$ absorption spectrum consists of the $P_{4d}^{(Pd)}$ and $P_{5s}^{(Pd)}$. Therefore, this experimental spectrum must be compared with $I(p \rightarrow d)P_{4d}^{(Pd)} + I(p \rightarrow s)P_{5s}^{(Pd)}$, where $I(p \rightarrow d)$ and $I(p \rightarrow s)$ are oscillator strengths for the dipole-allowed

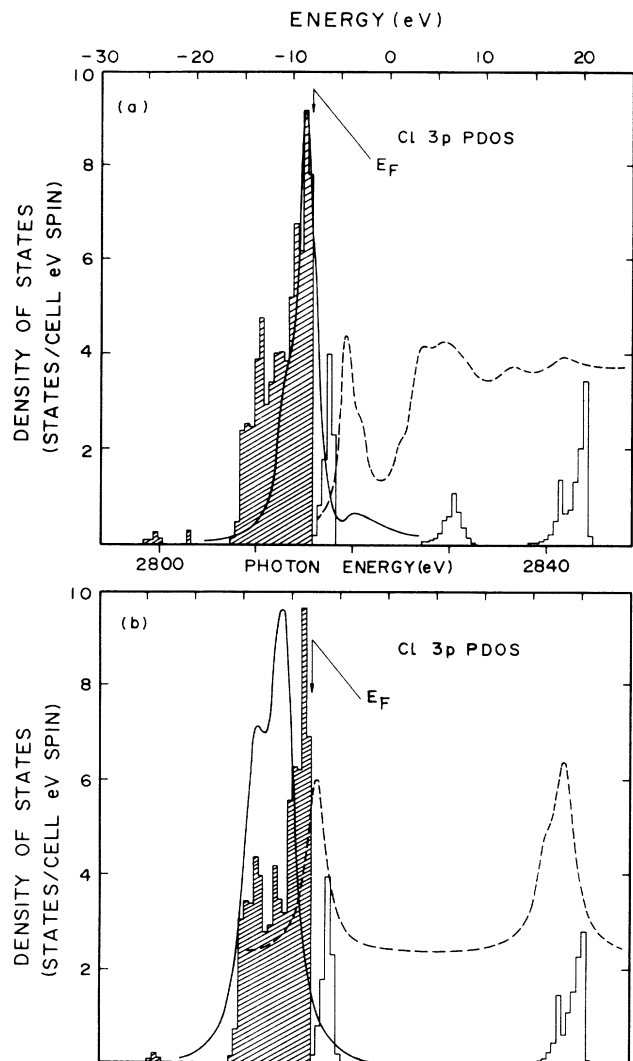


FIG. 4. Partial density of states (PDOS) for $3p$ orbital of $\text{Cl}^{0.6-}$ ion in K_2PdCl_6 as a function of energy measured from vacuum level. $\text{Cl } K\beta$ emission (solid curves) and $\text{Cl } K$ absorption (dashed curves) spectra obtained from the experiment and from the MO calculations based on the SCCXH method are drawn in (a) and (b), respectively. The PDOS illustrated in (b) is the result obtained by neglecting the K^+ ions.

transitions from the $\text{Pd } 2p$ orbital to the $\text{Pd } 4d$ and $\text{Pd } 5s$ orbitals. We have numerically calculated the $I(p \rightarrow d)$ and $I(p \rightarrow s)$, and found the ratio $I(p \rightarrow s)/I(p \rightarrow d)$ to be an order of 10^{-2} , so that the contribution of $P_{5s}^{(\text{Pd})}$ to the $\text{Pd } L_3$ absorption is very small as compared with that of the $P_{4d}^{(\text{Pd})}$. The band-structure calculation gives the energy separation (5.0 eV) between the main peak of the $\text{Pd } L\beta_{2,15}$ emission spectrum and the first peak of the $\text{Pd } L_3$ absorption spectrum, which is in good agreement with the experiment (4.75 eV, Ref. 1). For Cl spectra, however, its agreement is rather poor. The band-structure calculation [Fig. 4(a)] for the $\text{Cl } K\beta$ emission predicts a wider width than the experimental result, although it reproduces qualitatively the observed spectral shape. From this observation, it is thought that our band-structure cal-

ulation describes more adequately the property associated with the Pd metal than that associated with the Cl anion. Here, we should mention a possible reason why such an unbalanced situation takes place. Our band-structure calculation contains an adjustable parameter G used for the evaluation of the Hamiltonian matrix element [see Eq. (4) in Ref. 9]. The value of G , strictly speaking, should depend on quantum states for atoms on the different kinds of sites. Throughout the present paper, however, we have treated the parameter G as an isotropic value of 1.75 for simplicity. We think that this simplification may be inadequate to the Cl spectra. In order to clarify this point, we are now investigating band structures for well-studied CuX and AgX ($X = \text{Cl}, \text{Br},$ and I) crystals, by the XHTB method.¹⁵

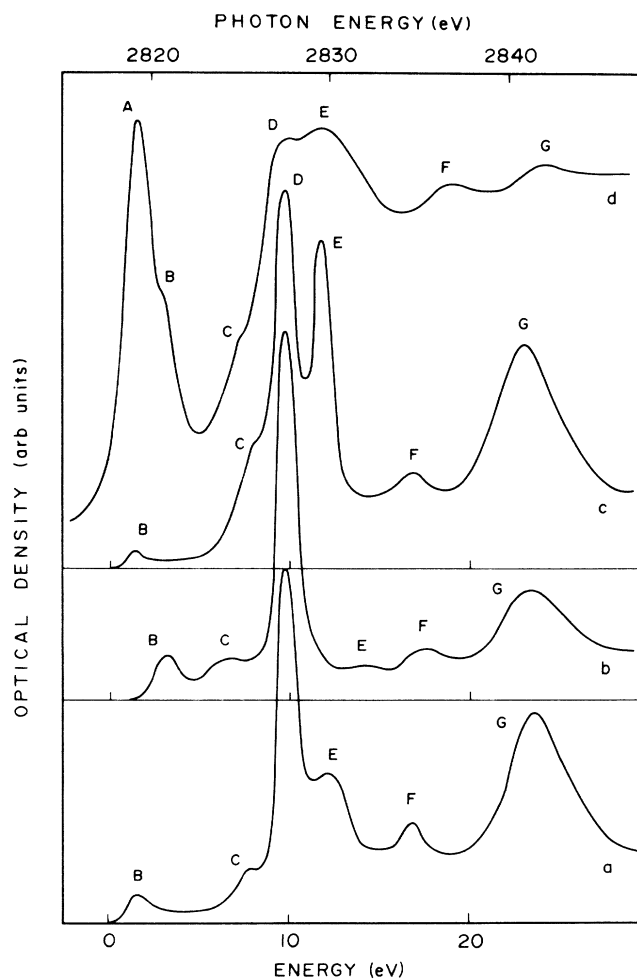


FIG. 5. $\text{Cl } K$ XANES spectra calculated for K_2PdCl_6 . Spectra *a*, *b*, and *c* are calculated under the three different conditions as follows: for spectrum *a*, the self-consistent charge (SCC) is used for the ionicities of the K , Pd , and Cl ions and the calculation is carried out with no core hole; for spectrum *b*, the formal charge is used and the effect of a core hole is taken into account by using the Cl^- ion; and for spectrum *c*, the SCC is used and the core-hole effect is considered by using the $\text{Cl}^{0.6-}$ ion. Spectrum *d* is the experimental result for $\text{Cl } K$ absorption of K_2PdCl_6 crystal.

An appreciable difference between the PDOS's in Figs. 3(a) and 3(b) and in Figs. 4(a) and 4(b) is an appearance of the density of states around 5 eV in Figs. 3(a) and 4(a), which is due to contributions of K^+ ions. We should note that the PDOS's [Figs. 3(b) and 4(b)] obtained by neglecting the K^+ ions correspond well to the x-ray-absorption and -emission spectra calculated from the MO results, except for a slight shift of the positions of the corresponding peaks.

We have so far described the results for the band structure obtained by using the SCC. Here, we would like to comment on results calculated when the formal charge is used. These results were poor as compared with those for the SCC. Particularly, the energy separation between the main peak of the Pd $L\beta_{2,15}$ emission and the first peak of

the Pd L_3 absorption spectra was far from the experimental result, being about 5 times as large as the latter. This indicates that the present study of the band structure confirms the SCC for the K_2PdCl_6 crystal obtained by our previous MO calculation.¹

B. Cl K XANES

Here, we are concerned with the Cl K XANES spectrum which is drawn by the dashed curve in Fig. 4(a). Its first peak can be predicted by both the MO and band-structure calculations, but the structures following the first peak cannot be done. So, we apply the MS theory, which describes transitions to continuum states adequately, to the present problem.

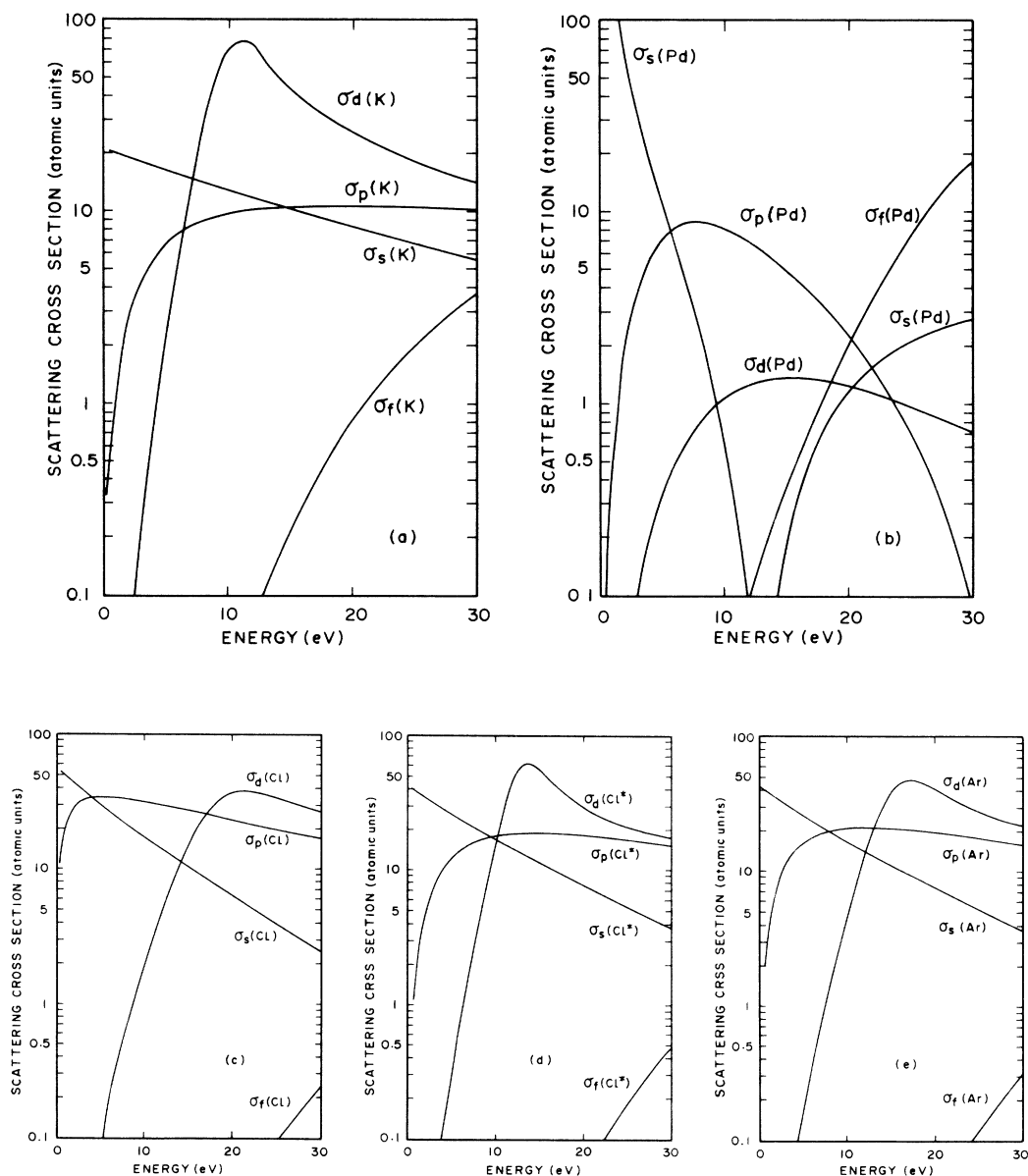


FIG. 6. Energy dependence of the partial-wave scattering cross section $\sigma_l(\mu)$ ($l=s, p, d,$ and f) for (a) $\mu=K^+$, (b) $\mu=Pd^{1.6+}$, (c) $\mu=Cl^{0.6-}$, (d) $\mu=Cl^*$, and (e) $\mu=Ar^{0.6-}$ ions, where Cl^* means the K x-ray-absorbing $Cl^{0.6-}$ ion.

The Cl K XANES spectra calculated on the basis of the MS theory for three different conditions are shown in Fig. 5, where they are compared with the experimental spectrum denoted by d . Spectrum a was calculated by using a self-consistent charge (SCC) for ionicities of the K, Pd, and Cl ions and with no core-hole effect; spectrum b by using the formal charge and by taking into account the effect of a core-hole through the electron configuration of K x-ray-absorbing Cl^- ion described in Sec. II; and spectrum c by using the SCC and by taking into account the core-hole effect by use of the K x-ray-absorbing $\text{Cl}^{0.6-}$ ion. The origin of the energy of the calculated spectra is the MT zero, which is -9.41 eV for spectrum a , -7.79 eV for spectrum b , and -9.41 eV for spectrum c , measured from the vacuum level.

All the calculated spectra a , b , and c show the observed structures B , C , D , E , F , and G , which follow the first peak A . We see that the structure E notably changes depending on calculational conditions, but the other structures remain almost the same. From the comparison of these three spectra with the experiment, we can conclude that spectrum c is best fitted to the experimental spectrum. This conclusion is consistent with the result for the ionicities of the K, Pd, and Cl ions, which is obtained from the MO and band-structure studies.

Here, we consider the contribution of the scattering cross section of the partial f wave, which is neglected in the present calculation. The scattering cross sections $\sigma_l(\mu)$ ($l=s, p, d, \text{ and } f$) are illustrated in Figs. 6(a)–6(d) for $\mu=\text{K}^+, \text{Pd}^{1.6+}, \text{Cl}^{0.6-}$, and K x-ray-absorbing $\text{Cl}^{0.6-}$ (Cl^*) ions, respectively, along with that for the $\text{Ar}^{0.6-}$ ion [Fig. 6(e)]. In the present MS calculations we used $l_{\text{max}}=2$, namely the effect of the partial f wave was not included. The result for the $\sigma_f(\text{K})$ and $\sigma_f(\text{Pd})$ in Figs. 6(a) and 6(b) indicates that the effect of the partial f wave cannot be neglected in the energy region above 15 eV. Unfortunately, from the reason mentioned in Sec. II we could not do the MS calculation including the partial f wave. We believe that the calculation including the partial f wave would give a result which is much closer to the experiment, particularly in the high-energy region.

Finally we comment on the effect of a core hole upon

the scattering cross sections. The scattering cross sections for the Cl^* ion calculated by considering the core hole, $\sigma_l(\text{Cl}^*)$, show a behavior which is intermediate between those of the $\sigma_l(\text{K})$ [Fig. 6(a)] and the $\sigma_l(\text{Cl})$ [Fig. 6(c)] for $l=s, p, d, \text{ and } f$. This fact leads us to conjecture that the scattering cross sections for the MT potential of Cl^* ion are similar to those of Ar located between Cl and K in the Periodic Table. In order to show it clearly, we have actually calculated the $\sigma_l(\text{Ar})$ by using the MT potential for the $\text{Ar}^{0.6-}$ ion, whose electron configuration is $(1s^2 2s^2 2p^6 3s^2 3p^6 4p^{0.6})$. We see that the $\sigma_l(\text{Cl}^*)$ and $\sigma_l(\text{Ar})$ in Figs. 6(d) and 6(e) really show a very similar dependence on the energy. This fact qualitatively supports the availability of the so-called $Z+1$ potential method,^{16,17} which is usually used to take into account the core-hole effect in the calculation of the XANES spectra based on the MS theory.

IV. SUMMARY

We have reported the first calculation of the band structure for the K_2PdCl_6 crystal, and found that the calculation based on the extended Hückel tight-binding method gives fairly reasonable agreement with the x-ray-emission spectra and the first peak of the absorption spectrum. It has also been shown that the multiple structures following the first peak in the Cl K absorption spectrum of the K_2PdCl_6 crystal can be reasonably reproduced by the multiple-scattering approach, when the self-consistent charge (SCC) obtained from our previous molecular-orbital (MO) calculation is used. The conclusion in the present study is that in order to understand the electronic properties of the K_2PdCl_6 crystal, it is essential to take the SCC as ionicities of K, Pd, and Cl ions. This suggests that electronic properties for K_2PtCl_6 -type crystals listed in the table of Wyckoff¹⁴ should be studied starting from the SCC obtained by MO calculations.

We hope that an experimental study, which clarifies the total density of states presented in the present paper, will be made in the near future.

¹M. Kitamura, C. Sugiura, and S. Muramatsu, Phys. Rev. B **39**, 10 288 (1989).

²M. Kitamura, S. Muramatsu, and C. Sugiura, Phys. Rev. B **33**, 5294 (1986).

³M. Kitamura, C. Sugiura, and S. Muramatsu, Solid State Commun. **62**, 663 (1987).

⁴M. Kitamura, S. Muramatsu, and C. Sugiura, Phys. Status Solidi B **142**, 191 (1987).

⁵M. Kitamura, S. Muramatsu, and C. Sugiura, Phys. Rev. B **37**, 6486 (1988).

⁶M. Kitamura, C. Sugiura, and S. Muramatsu, Solid State Commun. **67**, 313 (1988).

⁷M. Kitamura, C. Sugiura, and S. Muramatsu, Phys. Status Solidi B **149**, 791 (1988).

⁸M. Kitamura, S. Muramatsu, and C. Sugiura, Physica B (Am-

sterdam) **158**, 608 (1989).

⁹M. Kitamura and S. Muramatsu, Phys. Rev. B **41**, 1158 (1990).

¹⁰M. Wolfsberg and L. Helmholz, J. Chem. Phys. **20**, 837 (1962).

¹¹F. Herman and S. Skillman, *Atomic Structure Calculations* (Prentice-Hall, Englewood Cliffs, NJ, 1963).

¹²K. Schwarz, Phys. Rev. B **5**, 2466 (1972).

¹³H. M. Evjen, Phys. Rev. **39**, 675 (1932).

¹⁴R. W. G. Wyckoff, *Crystal Structures* (Interscience, New York, 1951), Vol. 3.

¹⁵S. Muramatsu and M. Kitamura (unpublished).

¹⁶P. A. Lee and G. Beni, Phys. Rev. B **15**, 2862 (1977).

¹⁷P. J. Durham, J. B. Pendry, and C. H. Hodges, Solid State Commun. **38**, 159 (1981).